IEICE TRANS. COMMUN., VOL.E89–B, NO.1 JANUARY 2006

PAPER

Polarimetric Scattering Analysis for a Finite Dihedral Corner Reflector

Kei HAYASHI[†], *Student Member*, **Ryoichi SATO**[††a)], **Yoshio YAMAGUCHI**[†††], *and* **Hiroyoshi YAMADA**[†††], *Members*

SUMMARY This paper examines polarimetric scattering characteristics caused by a dihedral corner reflector of finite size. The dihedral corner reflector is a basic model of double-bounce structure in urban area. The detailed scattering information serves the interpretation of Polarimetric Synthetic Aperture Radar (POLSAR) data analysis. The Finite-Difference Time-Domain (FDTD) method is utilized for the scattering calculation because of its simplicity and flexibility in the target shape modeling. This paper points out that there exists a stable double-bounce squint angle region both for perfect electric conductor (PEC) and dielectric corner reflectors. Beyond this stable squint angular region, the scattering characteristics become completely different from the assumed response. A criterion on the double-bounce scattering is proposed based on the physical optics (PO) approximation. The detailed analyses on the polarimetric index (co-polarization ratio) with respect to squint angle and an experimental result measured in an anechoic chamber are shown.

key words: *finite dihedral corner reflector, double-bounce scattering, radar polarimetry, POLSAR*

1. Introduction

Polarimetric Synthetic Aperture Radar (POLSAR) has been attracting attention in microwave remote sensing [1], [2]. POLSAR provides us scattering matrix over vast terrain area which can be used to monitoring, surveillance and environmental issues. One of the most important applications in POLSAR data is classification or identification of target. The classification is based on decomposition on physical scattering nature. It has been reported that there exist three main scattering mechanisms, i.e., surface scattering, double-bounce scattering and volume scattering [3], [4]. Recently, the fourth component is proposed in Ref. [5].

Here we focus on the double-bounce scattering. The scattering is caused by for example road surface and building wall in urban area. These structures can be seen in various man-made targets with respect to radar wavelength. However, in actual POLSAR image analysis, the double-bounce scattering is not always observed when the structure is aligned not orthogonal to radar line of sight. It is, therefore, very important to investigate the angular dependency of the backscattering from the structure. Although the physical reflection may be simple, however, a question on the scattering characteristics comes out. How much degree does the structure act as double-bounce scattering target with respect to squint and/or incident angle? How much size with respect to wavelength is enough for double-bounce target? How does the total reflection power (radar cross section: RCS) change with angle? Since the double-bounce scattering is modeled simply as the scattering matrix $[S] = \begin{bmatrix} 1 & 0 \\ 0 & -1 \end{bmatrix}$ in various decomposition methods [3]–[5], these questions are essential to understanding and decomposition of POLSAR data. These points are not investigated in the previous literatures [6]–[8].

In this paper, therefore, we model the double-bounce structure as a composite of two thick plates (a finite dihedral corner reflector) as shown in Fig. 1, and carry out polarimetric scattering analysis by using the Finite-Difference Time-

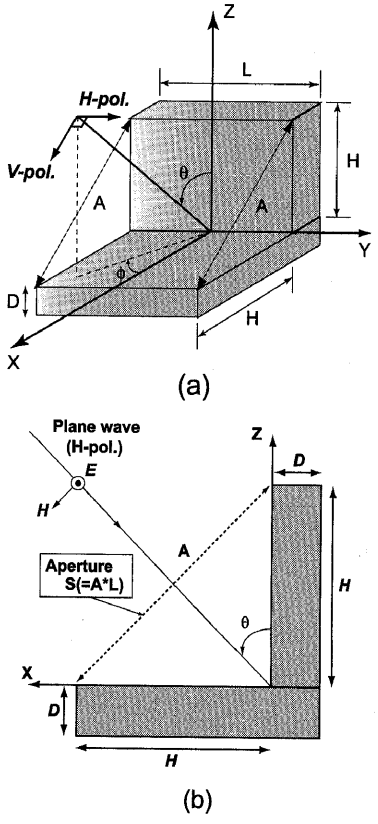

Fig. 1 Geometry of the problem (θ: look angle, ϕ: squint angle). (a) A finite dihedral corner reflector, (b) Side view of the dihedral reflector.

Manuscript received May 17, 2005.
Manuscript revised August 23, 2005.

[†]The author is with the Graduate School of Science and Technology, Niigata University, Niigata-shi, 950-2181 Japan.
[††]The author is with the Faculty of Education and Human Sciences, Niigata University, Niigata-shi, 950-2181 Japan.
[†††]The authors are with the Department of Information Engineering, Niigata University, Niigata-shi, 950-2181 Japan.
a) E-mail: sator@ed.niigata-u.ac.jp

DOI: 10.1093/ietcom/e89–b.1.191

Domain (FDTD) method [9]. The validity of the FDTD analysis for the finite model is first assessed by comparing with the experimental result measured in an anechoic chamber. After that, the squint angular dependency of both the monostatic RCS and the co-polarization ratio is investigated, since the squint angle is a critical parameter for the dihedral structure. It is found from the FDTD analysis that there exists a squint angular region where the phase of co-polarization ratio is stable even though the RCS changes drastically within the main lobe. This squint angular region can be observed not only for perfect electric conductor (PEC) but also for dielectric corner reflector. The phase behavior may be considered as one of the double-bounce scattering features. From the detailed examination based on the physical optics (PO) approximation for large aperture target model [10], [11], a criterion of the applicable squint angular range with the stable double-bounce scattering is finally proposed by considering the feature of the function $\sin X/X$.

Section 2 briefly introduces the scattering matrix and the FDTD procedure in the polarimetric scattering analysis. In Sect. 3, some numerical results and the detailed consideration on the scattering features for angular change are provided.

2. Polarimetric Scattering Analysis

2.1 Scattering Matrix in Radar Polarimetry

In a polarimetric electromagnetic wave scattering problem, when horizontal (H) and vertical (V) linear polarized plane waves, E_H^t and E_V^t, impinge on a target, the scattered wave contribution $\boldsymbol{E}^s$ can be expressed as

$$\boldsymbol{E}^s = \begin{bmatrix} E_H^s \\ E_V^s \end{bmatrix} = \begin{bmatrix} S_{HH} & S_{HV} \\ S_{VH} & S_{VV} \end{bmatrix} \begin{bmatrix} E_H^t \\ E_V^t \end{bmatrix} = [S]\boldsymbol{E}^t, \quad (1)$$

where the subscript for each element in the 2×2 matrix part, HH, HV, VH, VV, stands for the relationship of the polarization state between the scattered and transmitted waves. For example, S_{VH} is the vertical polarized scattering component for a horizontal polarized transmission. The 2×2 matrix

$$[S] = \begin{bmatrix} S_{HH} & S_{HV} \\ S_{VH} & S_{VV} \end{bmatrix} \quad (2)$$

is called the Sinclair scattering matrix, which is considered as a scattering operator due to the existence of the target for an arbitrary input $\boldsymbol{E}^t$. Also, in order to estimate various polarimetric properties, $[S]$ can be transformed to several matrix forms, the Mueller matrix, the Covarience matrix, the Coherency matrix, and so on. Therefore, it is very important in the first process of polarimetric analysis to obtain and evaluate the scattering matrix $[S]$ for the target.

2.2 FDTD Analysis for a Finite Dihedral

As depicted in Fig. 1, we will consider polarimetric scattering problem when H or V linear polarized plane wave impinges on a finite dihedral corner reflector. The definition of H or V polarization is shown in Fig. 1(a). The plane wave is transmitted from a radar and incident on the target as shown in Fig. 1(b).

In this paper, the Finite-Difference Time-Domain (FDTD) method [9] is employed to obtain the scattering matrix for the finite dihedral corner reflector. The advantage of the FDTD method is its flexibility in target shape modeling and specification of material constant. It is possible to examine "edge effect" in the scattered field by simple modification of finite corner reflector shape and size. Incident wave direction can be easily changed. This yields polarimetric scattering characteristics at any look and squint angles. The scattering matrix $[S]$ is obtained by the far field transformation. The fundamental parameters of the FDTD simulation used here are shown in Table 1.

Table 1 Parameters in FDTD simulation.

Analytical region	$350 \times 350 \times 350$ cells
Cubic cell size Δ	0.01 m
Time step Δt	1.925×10^{-11} s
Incident pulse	Lowpass Gaussian pulse
Absorbing boundary condition	Mur 2nd

In the next section, we will examine the co-polarized backscattering characteristics for the finite dihedral, for which the magnitude of co-polarized component is much larger (more than 20 dB) than that of cross-polarized one. However, we must pay attention to very small scattering contribution such as cross-polarized backscattering, because the present FDTD simulation may not have enough precision for such case due to the accuracy limitation of Mur's absorbing boundary condition [9].

3. Numerical Results and Discussion

To find out particular polarimetric scattering characteristics by the finite dihedral, FDTD calculations have been extensively carried out.

The first step is to check the accuracy of the FDTD analysis. Let us compare the FDTD numerical result with the measurement one for the finite PEC dihedral model. In the FDTD analysis, the target dimension is chosen as L=10.0λ (2.5 m), H=10.0λ (2.5 m) and D=0.04λ (0.01 m) for the operating frequency 1.2 GHz. While, the polarimetric measurement has been carried out in an anechoic chamber at 10 GHz frequency. The dimension of the chamber is about 3 m × 3 m × 2.5 m. In the measurement, a frequency scale model is employed. The size (L=0.3 m, H=0.3 m and D=0.003 m) at 10 GHz is almost equivalent to that of the FDTD analysis at 1.2 GHz. Table 2 shows the co-polarization ratio S_{VV}/S_{HH} for both the FDTD and the measured results at normal squint angle $\phi = 0°$. We can see good agreements both for amplitude $|S_{VV}/S_{HH}|$ and phase $\angle(S_{VV}/S_{HH})$. Hence, the validity of the FDTD analysis has been confirmed for the finite target.

For the finite dihedral structure, the double-bounce

Table 2 Comparison of co-polarization ratio S_{VV}/S_{HH} for scaled PEC model with $L = H = 10\lambda$ ($\theta = \theta_i = 45°$).

	Co-pol.ratio	Finite PEC dihedral	
		FDTD (1.2 GHz)	Measurement (10 GHz)
$\phi = 0°$	Amplitude	0.99	1.07
	Phase [deg.]	177	179

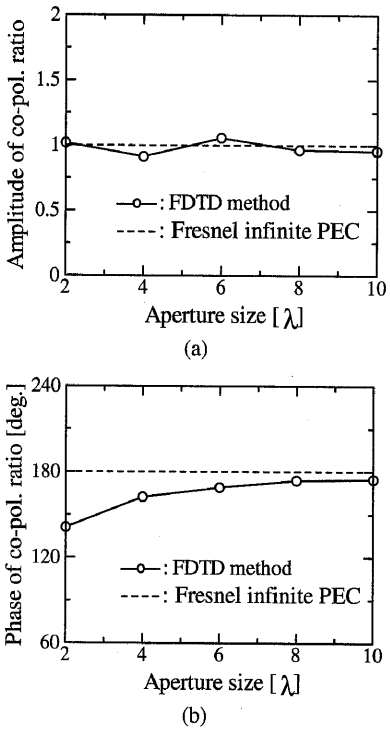

Fig. 2 Co-polarization ratio S_{VV}/S_{HH} for aperture size variation ($\theta = \theta_i = 45°, \phi = \phi_i = 0°$). (a) Amplitude, (b) Phase.

scattering feature may be dependent on the aperture size A with respct to the radar wavelength, where A is defined in Fig. 1. If the aperture size A is small, the edge effect will act on the value of co-polarization ratio because the cross-polarization component may be produced at the aperture edge. So let us next show the aperture size A dependency of the co-polarization ratio S_{VV}/S_{HH}. In Fig. 2, the aperture is chosen as $S = A \times A$ ($L = A$) and the other parameters are $D = 2.4\lambda$ (0.6 m) at 1.2 GHz, $\theta = \theta_0 = 45°$ and $\phi = \phi_0 = 0°$. For a reference, the result for infinite PEC dihedral is also included in the figure. From Figs. 2(a) and (b), one can observe that when the aperture size becomes larger than 8λ, the amplitude of the co-polarization ratio tends to be almost 1, and the phase approaches to 180 degrees, respectively. This polarimetric behavior is very similar to that for infinite PEC dihedral. It is, therefore, considered that the edge effect can be neglected for aperture size $A \geq 8\lambda$. Taking into account this consideration, the dimension of the dihedral will be chosen as $A \geq 8\lambda$ in the following FDTD calculations.

Now, let us consider the polarimetric characteristics for angular variation. Figure 3 shows the monostatic RCS values from the finite PEC dihedral for squint angle ϕ variation. Here, the look angle θ is not critical parameter for the structure, so it is constant as $\theta = \theta_i = 45°$. Each dimension

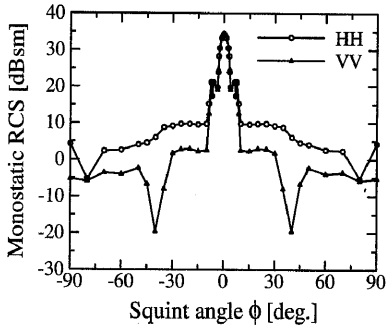

Fig. 3 Monostatic RCS from a PEC dihedral reflector for squint angle ϕ variation ($\theta = \theta_i = 45°$).

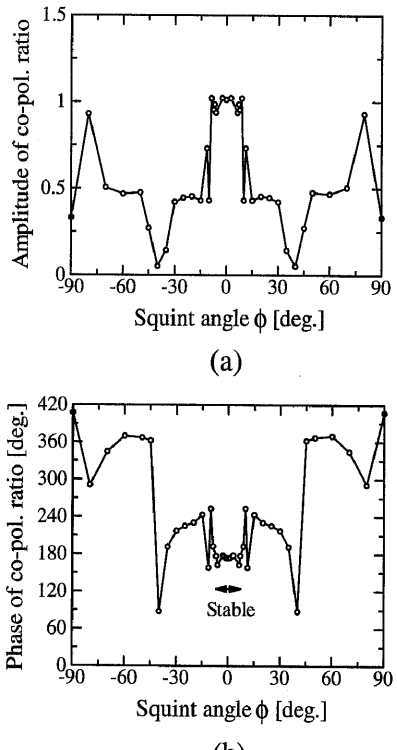

Fig. 4 Co-polarization ratio S_{VV}/S_{HH} from a PEC dihedral reflector for squint angle ϕ variation ($\theta = \theta_i = 45°$). (a) Amplitude, (b) Phase.

size of the PEC target is L=8.4λ (2.10 m), H=5.7λ (1.42 m) and D=2.4λ (0.60 m) at 1.2 GHz frequency, where the corresponding aperture size A is about 8λ. One can observe that for each polarization, the monostatic RCS in $|\phi| < 5°$ keeps relatively strong value, compared to the further oblique region $|\phi| > 5°$. Strong back scattering is considered as one of the particular double-bounce scattering features, so that one may be able to regard the angular region $|\phi| < 5°$ as the double-bounce scattering angular region.

For more detailed polarimetric evaluation, let us next examine the co-polarization ratio S_{VV}/S_{HH}. Figure 4 shows the co-polarization ratio of the finite PEC dihedral for the squint angular change, where the dimension size here is as same as that in Fig. 3. In Fig. 4(a), the amplitude $|S_{VV}/S_{HH}|$ is close to about 1 when $|\phi| < 5°$. With the further increase of the aspect angle, $|S_{VV}/S_{HH}|$ is rapidly reduced down to

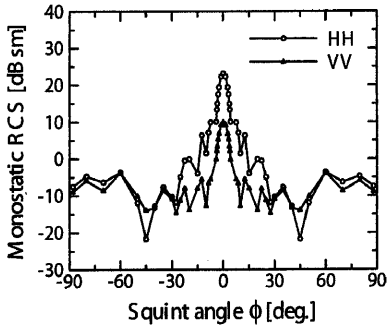

Fig. 5 Monostatic RCS from a dielectric dihedral reflector for squint angle ϕ variation ($\theta = \theta_i = 45°$).

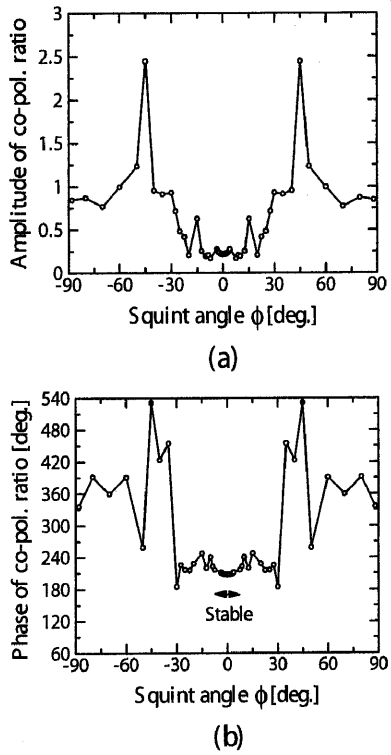

Fig. 6 Co-polarization ratio S_{VV}/S_{HH} from a dielectric dihedral reflector for squint angle ϕ variation ($\theta = \theta_i = 45°$). (a) Amplitude, (b) Phase.

about 0.5. Also, it is observed in Fig. 4(b) that the phase $\angle(S_{VV}/S_{HH})$ keeps almost constant value about 180° in the angular region $|\phi| < 5°$. From these polarimetric features, it is again verified that the squint angular region $|\phi| < 5°$ is considered as the double-bounce scattering angular region.

Furthermore, Figs. 5 and 6 illustrate the FDTD results for a dihedral corner reflecor composed of dielectric plates. In the FDTD calculations, the same dimension size is used. The relative permittivity ε_r and the conductivity σ of the material are chosen as 4.0 and 0.00667, respectively.

Figure 5 shows the monostatic RCS value from the dielectric dihedral reflector for the squint angular variation. In comparison with that for the large squint angular region $|\phi| > 5°$, the RCS within $|\phi| < 5°$ shows relatively strong value. However, the value is always smaller than that for PEC reflector model.

For the co-polarization ratio, it can be seen from

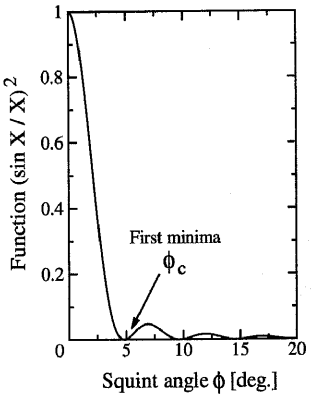

Fig. 7 The function $(\sin X/X)^2$ for the angle ϕ variation ($X = kL\cos\theta\sin\phi$, $L = 8.4\lambda$, $\theta = \theta_i = 45°$, $f = 1.2$ GHz).

Fig. 6(a) that the amplitude $|S_{VV}/S_{HH}|$ is not close to 1.0 even for the small angular region $|\phi| < 5°$. However, the phase $\angle(S_{VV}/S_{HH})$ is roughly constant in $|\phi| < 5°$, even though it undergoes small oscillation change (Fig. 6(b)). Taking into account these discussions, the double-bounce scattering angular region for dielectric dihedral reflector may be defined as follows: 1) The double-bounce scattering region is the squint angular range with relatively strong back scattering, 2) The phase of co-polarization ratio tends to be roughly stable in the angular region, although the amplitude is not always close to 1.0.

Finally, we propose a criterion for double-bounce scattering angular region based on the numerical FDTD results and physical optics (PO) approximation. Since the troublesome edge contributions are negligible for large aperture case as A (and L) $\geq 8\lambda$ at $\phi \sim 0$, the double-bounce scattered field by the finite dihedral may be considered as the PO approximate one due to the equivalent uniform current distribution on the aperture S ($= A \times L$) of the target [10], [11]. The approximate field is proportional to the function $\sin X/X$, where $X = kL\cos\theta\sin\phi$, k is the wave number. Figure 7 displays the angle ϕ dependency of the intensity $(\sin X/X)^2$, where $L = 8.4\lambda$, $\theta = 45°$. In comparison with the above results for the finite dihedral reflectors, one can immediately recognize that the derived double-bounce scattering regions both for the PEC and dielectric reflectors include the angle, $\phi_c = 4.83°$, for the first minima of $(\sin X/X)^2$ in Fig. 7. This angle ϕ_c is derived for $X = \pi$, i.e.,

$$\phi_c = \sin^{-1}(\lambda/2L\cos\theta). \tag{3}$$

In large squint angular region over the first minima, the assumed uniform distribution condition on the aperture may not be satisfied, so that only for small angle $\phi \leq \phi_c$, the approximation $\sin X/X$ can include the double-bounce scattering contribution with the stable phase feature. To confirm the validity of Eq. (3), we made additional FDTD calculations not only for different size parameters but also for different conductivity under the condition A (and L) $\geq 8\lambda$. It was verified from the results that the double-bounce scattering region is dependent on the lateral size parameter L of the model, and independent of other parameters. It is, therefore,

concluded that the criterion of the applicable double-bounce scattering angular region can be given by the critical squint angle ϕ_c obtained by Eq. (3).

4. Conclusion

In this paper, polarimetric electromagnetic wave scattering analysis for a finite dihedral corner reflector has been carried out by using the FDTD method. It has been found from the extensive numerical calculations that there exists a double-bounce squint angular region where the phase of the co-polarization ratio is stable. A criterion of the applicable squint angle region has been proposed by a consideration based on the physical optics approximation for large aperture target.

As a future development, taking into account the polarimetric angular feature of the discussed double-bounce scattering, the accuracy improvement of the decomposition method based on three- or four-component scattering model [3]–[5] will be considered in actual POLSAR image analysis. We also intend to investigate the cross-polarized backscattering for angular variation.

Acknowledgments

The authors express their sincere appreciation to Professor H.J. Eom, for helpful discussions, and to the anonymous reviewers for their useful comments. This research was partially supported by a Scientific Research Grant-In-Aid from the Ministry of Education, Culture, Sports, Science and Technology, Japan, and carried out in cooperation with Center for Information and Communication Research, Niigata University.

References

[1] F.M. Henderson and A.J. Lewis, ed., Principles & Applications of Imaging Radar 3rd ed., Manual of Remote Sensing, vol.3, John Wiley & Sons, 1998.
[2] B.A. Cambell, Radar Remote Sensing of Planetary Surfaces, Cambridge Univ. Press, 2002.
[3] A. Freeman and S.L. Durden, "A three-component scattering model for polarimetric SAR data," IEEE Trans. Geosci. Remote Sens., vol.36, no.3, pp.963–973, May 1998.
[4] T. Moriyama, S. Uratsuka, T. Umehara, H. Maeno, M. Satake, A. Nadai, and K. Nakamura, "Polarimetric SAR image analysis using model fit for urban structures," IEICE Trans. Commun., vol.E88-B, no.3, pp.1234–1243, March 2005.
[5] Y. Yamaguchi, T. Moriyama, M. Ishido, and H. Yamada, "A proposal of four-component scattering model for polarimetric SAR image decomposition," IEICE Technical Report, A·P2004-132, Sept. 2004.
[6] Z.-G. Xia and F.M. Henderson, "Understanding the relationship between radar response patterns and the bio- and geophysical parameters of urban areas," IEEE Trans. Geosi. Remote Sens., vol.35, no.1, pp.93–101, Jan. 1997.
[7] Y. Dong, B. Forster, and C. Ticehurst, "Radar backscatter analysis for urban environments," Int. J. Remote Sensing, vol.18, no.6, pp.1351–1364, 1997.
[8] G. Franceschetti, A. Iodice, and D. Riccio, "A canonical problem in electromagnetic backscattering from buildings," IEEE Trans. Geosi. Remote Sens., vol.40, no.8, pp.1787–1801, Aug. 2002.
[9] A. Taflove and S.C. Hagness, Computational Electrodynamics 2nd ed., Artech House, 2000.
[10] F.T. Ulaby, R.K. Moore, and A.K. Fung, Microwave Remote Sensing, Active and Passive, vol.1, Addison-Wesley Publishing, 1981.
[11] A. Ishimaru, Electromagnetic Wave Propagation, Radiation, and Scattering, Prentice Hall, 1991.

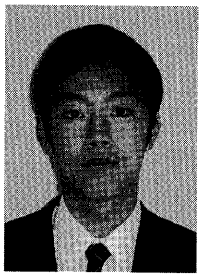

Kei Hayashi was born in Niigata, Japan, on April 23, 1980. He received the B.Ed. degree, and the M.E. degree in information engineering from Niigata University, Niigata, Japan, in 2003, and 2005, respectively. He was engaged in FDTD analysis for radar polarimetry. He is now with Mitsubishi Electric Corporation.

Ryoichi Sato received the B.S., M.S. and Ph.D. degrees in electrical engineering from Chuo University, Tokyo, Japan, in 1992, 1994 and 1997, respectively. Since April 1997, he has been with the Faculty of Education and Human Sciences, Niigata University, Japan, where he is currently an associate professor. In 2002, he was a Reserch Scholar at Polytechnic University, Brooklyn, NY. His current research interests are electromagnetic wave propagation, scattering and diffraction, and radar polarimetry. Dr. Sato is a member of IEEE.

Yoshio Yamaguchi received the B.E. degree in electronics engineering from Niigata University in 1976, and M.E. and Dr. Eng. degrees from Tokyo Institute Technology in 1978 and 1983, respectively. In 1988, he joined the Faculty of Engineering, Niigata University, where he is a professor. From 1988 to 1989, he was a Reserch Associate at University of Illinois at Chicago. His interests are in the field of propagation characteristics of electromagnetic waves in lossy medium, radar polarimetry, microwave remote sensing and imaging. Dr. Yamaguchi is a Fellow of IEEE.

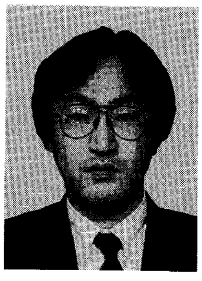

Hiroyoshi Yamada received the B.E., M.E., and Dr. Eng. degrees from Hokkaido University, Sapporo, Japan, in 1988, 1990 and 1993, respectively, all in electronic engineering. In 1993, he joined the Faculty of Engineering, Niigata University, where he is an associate professor. From 2000 to 2001, he was a Visiting Scientist at Jet Propulsion Laboratory, California Institute of Technology, Pasadena. His current interests involve in the field of array signal processing, radar polarimetry and interferometry, microwave remote sensing and imaging. Dr. Yamada is a member of IEEE.